

OVERLOAD INDUCED FATIGUE CRACK GROWTH AND  
SIGNIFICANCE OF RETARDATION ZONE

R.K. PANDEY and B.B. VERMA  
Department of Applied Mechanics,  
Indian Institute of Technology, Hauz Khas,  
New Delhi-110 016, India.

ABSTRACT

The behaviour of fatigue crack propagation has been studied in an Al-alloy and a steel on application of an overloading cycle. The crack acceleration during overloading cycle has been measured using scanning electron microscope (SEM) and electrical potential difference (EPD) techniques. The effects of overloading ratio (OLR), stress ratio (R) and  $\Delta K_I$  on crack acceleration have been investigated. The overload induced closure,  $K_{OP}^{OL}$  has been measured. The effects of various parameters on the size of retardation zones,  $a_D$  and  $a_D^*$  have been further studied. The size scale of retardation zones with respect to the overload monotonic plastic zone ( $2r_m^{OL}$ ) and the overload cyclic plastic zone ( $2r_C^{OL}$ ) has been rationalized based on the findings from present research as well as reanalysis of data from literature.

**KEYWORDS** - Retardation zone, Fatigue overloading,  
Overload plastic zone, Cyclic plastic zone,  
Crack closure, Fatigue crack growth rate.

INTRODUCTION

The structural components subjected to fatigue loading during service do encounter either random (variable amplitude loading or occasional overloading cycle in course of their life. Sometimes, the overloading cycles are purposely applied to produce some beneficial effects. Such overloads lead to retardation of a growing fatigue crack which may sometimes culminate into crack arrest. On the other hand, the overloading cycles could also lead to an acceleration of the growing fatigue crack which may prove dangerous in critical structures. To derive the maximum benefit from fatigue overload, it is imperative to understand the significance of post overload crack retardation zone as well as instantaneous crack growth behaviour on application of the overloading

cycle. This would help to optimise the 'level' and 'timing' of overload application to generate the desired effects. Also, the predictive capability of fatigue life can be further refined in this way.

The crack growth retardation due to overloading has been expressed by two parameters, namely, the retardation zone and delay cycles, ( $N_D$ ). Various models (Wheeler, 1972, Matsuoka and Tanaka, 1978, Willenborg, 1988) have been proposed in literature to characterize the phenomenon of retardation. However, the subject remains to be controversial. The present investigation is focussed upon the study of retardation zone and the role of various factors, eg., loading variables, crack tip plastic zones etc. are examined. In addition, the overloading induced crack growth acceleration is also studied. The investigation has been conducted in 2024-T3 Aluminium alloy (YS-375 MPa, TS-492 MPa and a Cr-Mo steel (YS-587 MPa, TS-723 MPa) which are used as aircraft structural materials.

### EXPERIMENTAL PROGRAMME

#### Materials and Test Specimens

The Al-alloy (Cu-4.5, Mg-1.5, Si-0.5, Zn-0.35, Mn-0.6) and Cr-Mo steel (C-0.26, Mn-0.50, Cr-0.99, Si-0.29, S-0.2, P-0.2) were available in sheet form of thicknesses 3.175 mm and 1.25 mm for the Al-alloy and the steel respectively. The centre cracked tension specimens of rectangular geometry (220 mm length, 85 mm width) were used with a crack starter hole (3.175 mm diameter) and a slit (4 mm length) in the centre. The specimens were well polished and fine lines were drawn parallel to the length of specimen to facilitate monitoring of crack propagation using travelling microscope.

#### Loading Parameters

The fatigue crack propagation study was conducted on Amsler Vibrophore machine in tension-tension mode under constant stress amplitude sinusoidal loading. The tests were conducted at ambient temperature (25-30°C) and at frequency of 75-100 Hz. The stress amplitude used during fatigue testing were about 12% and 20% of the yield strength for the aluminium alloy and the steel respectively. The tests were conducted at three different stress ratio  $R = 0.17, 0.30$  and  $0.44$  in both the alloys. For the study of overloading effects, the specimens were subjected to single overloading cycle. The overloading ratio (OLR) ( $\sigma^{OL}/\sigma_{max}$ ), applied to the specimens were 1.5, 1.7, 1.9, 2.1 and 2.3. The details of loading are reported elsewhere (Verma, 1993).

#### Fatigue Crack Growth Measurement

The fatigue crack growth was measured using EPD technique as well as the microscopic method. The current and potential probes were attached to the specimen at distances 40 mm and

17.5 mm respectively using copper screws. A current density of  $1.87 \times 10^{-8}$  A/m<sup>2</sup> was applied to Al-alloy and  $4.7 \times 10^{-8}$  A/m<sup>2</sup> to the steel sample through a regulated DC supply. The potential outputs on X-Y recorder were converted to crack length using calibration curves (Verma, 1993).

#### Crack Closure Measurement

The crack closure was measured using a clip gauge of 4 mm gage length and mounted at a distance of 1 mm behind the crack tip. The closure measurement was made at a low frequency (0.005 Hz) and the start of first non-linearity during loading or unloading was taken as the crack opening load. The closure loads were noted with the progress of loading cycles until the highest value of crack opening load was obtained which was used to compute the overload induced K-opening,  $K_{OP}^{OL}$ .

### RESULTS

A typical behaviour of fatigue crack growth rate (FCGR) da/dN on application of overloading cycle is shown in Fig. 1. Following the overloading cycle, immediate acceleration in FCGR was noticed and then subsequent retardation in post overload stage was obtained. An increase in basic stress intensity range,  $\Delta K$  resulted in a corresponding increase in crack growth acceleration (CGA) due to overloading. The effects of OLR and R on overload modified crack growth behaviour are also evident from the figure.

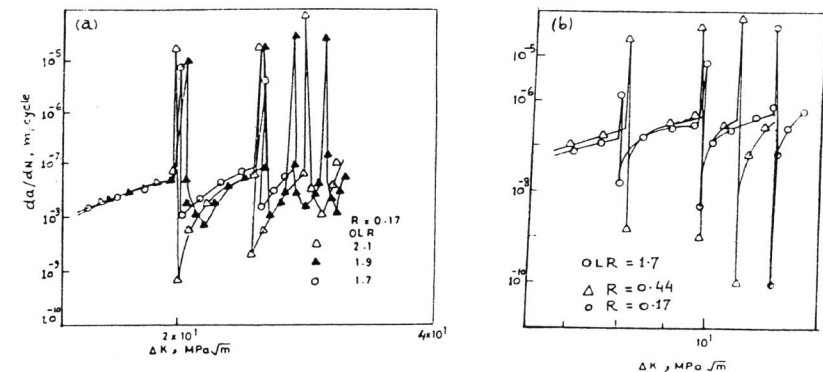


Fig. 1 FCGR as a Function of  $\Delta K$  in (a) Steel and (b) Al-Alloy

Post Overload Crack Opening SIF  $K_{Op}^{OL}$

Typical behaviour of overload crack opening SIF,  $K_{Op}^{OL}$  as a function of  $\Delta K$  is shown in Fig. 2. An increasing tendency of  $K_{Op}^{OL}$  with  $\Delta K$  was observed at a given R level. Also, a higher OLR was found to result in an increased value of  $K_{Op}^{OL}$  in both the alloys.

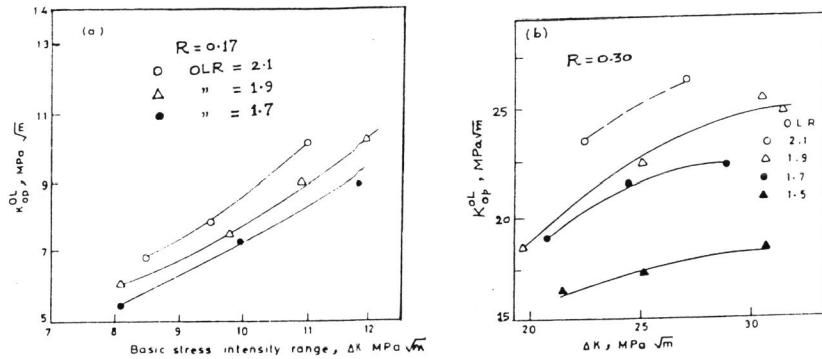


Fig. 2 Effect of  $\Delta K$  on  $K_{Op}^{OL}$  at Various OLR (a) Al-Alloy (b) Steel

DISCUSSION

Crack Growth Acceleration (CGA) Zone

From the nature of variation of overload induced FCGR as a function of  $\Delta K$  (Fig. 1), presence of following zones may be visualized: (i) Zone of crack growth acceleration ( $a^*$ ) (ii) Zone of crack growth deceleration (iii) The lowest FCGR (iv) Increasing FCGR in the retarded zone (v) Attainment of pre-overloading FCGR.

The crack growth acceleration zone ( $a^*$ ) is developed immediately on application of overload and has a dull and relatively rough surface in contrast to shining and smooth surface of the constant amplitude loading region. The difference between the texture of this zone and the constant amplitude loading region was more clearly evident in Al-alloy as compared to that of steel. The size of this zone as measured from the fracture surface in Al-alloy by using SEM at different level of  $\Delta K$  is reported in Table 1. The CGA zone was found to have a crescent shape. Since the CGA zone was not clearly discernable using SEM in case of steel, the length obtained through EPD technique is reported for steel. Besides

$a^*$  values, the table also shows the ratio  $r$  of the crack growth rate in CGA zone to the pre-overload constant amplitude FCGR. In both the alloys, generally, the CGA zone ( $a^*$ ) is found to increase with OLR at a given  $\Delta K$  and  $R$ . Also the  $a^*$  increases with  $\Delta K$  for a constant OLR and  $R$  value. The  $R$  has a similar effect on the size of CGA zone.

Table 1: Crack Growth Acceleration Zone ( $a^*$ ) in Al-Alloy and Steel

Alloy, R	OLR $\Delta K = 8 \text{ MPa} \sqrt{\text{m}}$	$a^*$ $\mu\text{m}$	$r$ $\times 10^2$	$a^*$ $\mu\text{m}$	$\Delta K = 10 \text{ MPa} \sqrt{\text{m}}$ $r \times 10^2$
Al-Alloy	1.7	21	1.0	40	1.4
	1.9	48	1.6	56	2.0
	2.1	72	3.0	77	2.7
0.30	1.9	73	-	71	-
		$\Delta K = 20 \text{ MPa} \sqrt{\text{m}}$		$\Delta K = 28 \text{ MPa} \sqrt{\text{m}}$	
Steel,	1.7	100	19	130	20
	1.9	115	26	180	26
	2.1	165	23	175	-
0.30	1.7	114	23	180	30
	1.9	180	54	-	-

$r$  = crack growth rate in CGA zone/pre-overload FCGR

The Crack Growth Rate in Acceleration Zone  $(da/dN)_i^{OL}$

The effect of OLR and  $\Delta K$  on the overload crack growth rate in the crack acceleration zone are presented in Fig.3. An increasing trend in  $(da/dN)_i^{OL}$  is noticed with  $\Delta K$  at a given level of OLR in both the alloys. Also with increasing OLR at a given  $\Delta K$ , the  $(da/dN)_i^{OL}$  continues to increase. It is interesting to note from Table 1 that on application of the overload in Al-alloy with OLR = 1.7, the crack growth rate is enhanced by about two orders of magnitude in the CGA zone as compared to that of the constant amplitude FCGR prior to overloading. On the other hand in case of steel the increase in crack growth rate in CGA zone is by three orders of magnitude.

The SEM microscopic examination of CGA zone exhibited presence of tear ridges and dimpled areas in case of steel. In addition, a number of voids and secondary cracks were also noticed. In Al-alloy the above zone was found to consist of deep voids and dimples along with tear ridges. The CGA zone resembles a typical stable crack growth zone of the monotonic loading situation. An enhancement of  $K_{Op}^{OL}$  due to increase of OLR appears to be main contributing factor for extension of this zone.

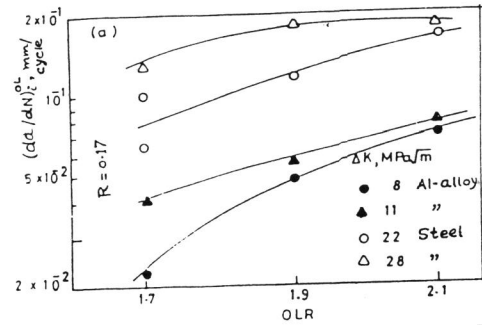


Fig. 3 Crack Growth Rate in Acceleration Zone against OLR in Al-Alloy and Steel

The greater enhancement of crack growth rate in CGA zone (i.e. higher ratio  $r$ ) in case of steel as compared to Al-alloy does also indicate that a high strength material when subjected to a relatively higher overloading cycle may pose a serious problem to the structure. A large tear zone may be formed which may rise to alarming level if multiple overloading cycles are applied.

Crack Retardation Zone

The crack retardation zone may be characterized by parameters  $a_D$  and  $a_D^*$  (as shown schematically in Fig. 4a where  $a_D$  is the overload affected total crack length and  $a_D^*$  is the crack length corresponding to the minimum crack growth rate.

Dependence of  $a_D$  and  $a_D^*$  on OLR: The effect of OLR on  $a_D$  and  $a_D^*$  has been discussed by several investigators (Bathias et al., 1978, Ranganathan et al., 1979, 1984, Robin et al., 1983). In the present investigation, the  $a_D$  values were found to increase with OLR in the beginning and beyond a certain level of OLR, it showed a saturating tendency at fixed level of  $R$  and  $\Delta K$  in both the alloys (Fig. 4,b,c). It may be noted that the increasing OLR causes an enhancement in  $K_{OL}$ . The  $K_{OL}$  level at which a decreasing trend in  $a_D$  was noticed lies around 26 and 61 MPa  $\sqrt{m}$  for the Al-alloy and steel respectively. The data (Drew et al., 1982, Rabin et al., 1983, Ranganathan et al., 1984, Vardar, 1988) were analysed and replotted (Fig. 5) to ascertain the dependence of  $a_D$  and  $a_D^*$  on OLR (or  $K_{OL}$ ). The results by and large fall along the line of observation from the present work. The functional variation of overload induced closure parameter,  $K_{Op}^{OL}$  against  $K_{OL}$  in these alloys further indicated a rising trend in  $K_{Op}^{OL}$

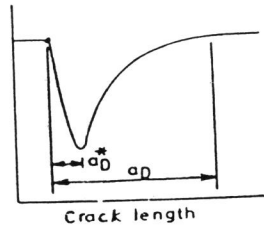


Fig. 4(a) Schematic Representation of  $a_D$  and  $a_D^*$

with  $K_{OL}$  upto 25 MPa  $\sqrt{m}$  and 65 MPa  $\sqrt{m}$  in the Al-alloy and the steel respectively. The coincidence of  $K_{OL}$  value for the  $a_D$  and  $K_{Op}^{OL}$  situations does positively indicate a dominant impact of overload induced closure on the size of retardation zone.

The Retardation Zone and Crack Tip Plastic Zone Size

Attempts have been made in literature to model the crack retardation behaviour incorporating the sizes of various plastic zones. Two most significant plastic zones at the crack tip are overload monotonic plastic zone ( $2r_m^{OL}$ ) and the overload cyclic plastic zone ( $2r_m^{OLC}$ ). The  $2r_m^{OL}$  were calculated corresponding to the existing stress state in test specimens using the following relationships

$$2r_m^{OL} = p[K_{OL}^2/\sigma_{ys}]^2 \tag{1}$$

where  $p = 1/\pi$  for plane stress and  $= 1/2\pi$  for mixed stress state. The results from present investigation are reported in Tables 2 and 3 showing  $a_D$  and  $a_D^*$  against the  $2r_m^{OL}$  and  $2r_m^{OLC}$ . A logarithmic relationship between  $a_D - 2r_m^{OL}$  and  $a_D - 2r_m^{OLC}$  was obtained as follows -

$$a_D = 1.82(2r_m^{OL})^{1.49} \quad \text{Al-alloy} \tag{2}$$

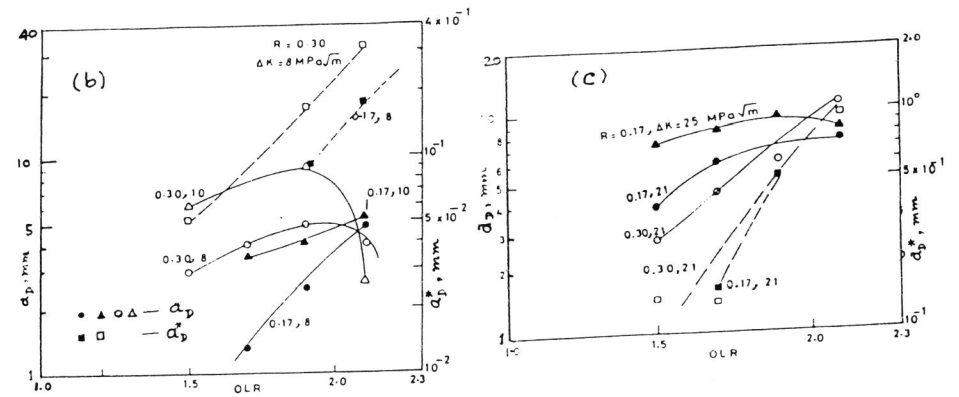


Fig.4 (b,c) Retardation Zones  $a_D$  and  $a_D^*$  vs. OLR in (b) Al-Alloy and (c) Steel (Present Investigation)

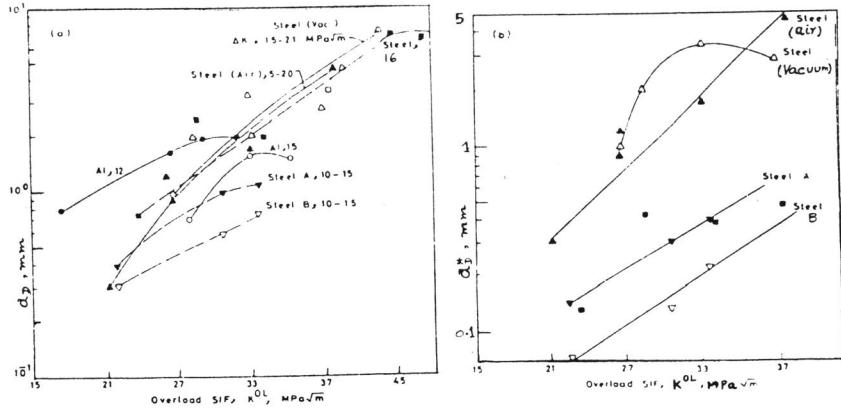


Fig. 5 Effect of Overloading  $K_{OL}$  on Retarded Crack Lengths (a)  $a_D$  and (b)  $a_D^*$  (Based on Literature Data)

$$a_D^* = 0.17(2r_m^{OL})^{2.52} \quad \text{Al-alloy} \quad (3)$$

$$a_D = 0.43(2r_m^{OL})^{2.00} \quad \text{Steel} \quad (4)$$

$$a_D^* = 0.04(2r_m^{OL})^{2.47} \quad \text{Steel} \quad (5)$$

Table 2: Retardation Zones ( $a_D$  and  $a_D^*$ ) and Overload Induced Monotonic Plastic Zone Size

Mats.,	$K_{OL}$ MPa $\sqrt{m}$	B/B $_{PE}$	$a_D$ , mm	$a_D^*$ , mm	$2r_m^{OL}$ ,mm (P.Stress)	$a_D/2r_m^{OL}$	$a_D^*/2r_m^{OL}$
Al-alloy	16.6	0.64	0.60	-	0.31	1.94	-
	21.5	0.40	2.20	0.18	1.01	2.20	0.18
	23.6	0.31	2.00	0.32	1.26	1.59	0.26
Steel	39.0	0.11	3.00	0.16	1.40	2.14	0.12
	45.2	0.08	1.40	0.14	1.88	0.74	0.08
	48.8	0.07	3.40	-	2.20	1.55	-
	52.5	0.06	3.05	-	2.55	1.20	-
	66.1	0.04	5.50	0.99	4.03	1.36	0.25

Table 3: Retardation Zones ( $a_D$  and  $a_D^*$ ) and Overload Induced Cyclic Plastic Zone Size

Mats.,	$K_{OL}$ MPa $\sqrt{m}$	B/B $_{PE}$	$a_D$ , mm	$a_D^*$ , mm	$2r_C^{OL}$ ,mm	$(a_D/2r_C^{OL})$	$(a_D^*/2r_C^{OL})$
Al-alloy	15.0	3.15	0.60	-	0.04	14.29	P.Strain
	19.8	1.81	2.20	0.18	0.07	30.99	2.51 "
	20.4	1.70	2.00	0.32	0.08	26.00	4.17 "
Steel	34.0	0.55	3.00	0.16	0.14	21.00	1.10 Mixed
	42.7	0.36	-	0.55	0.42	-	1.31 P.Stress
	44.6	0.32	3.05	-	0.46	6.61	- P.Stress
	57.0	0.20	5.50	0.99	0.76	7.35	1.31 P.Stress

The available data from literature for Al-alloy and steel (Drew et al., 1982, Robin et al., 1983, Ranganathan et al., 1984, Ward Close et al., 1989) were replotted and analysed. Based on all these observations it was ascertained that the  $a_D - 2r_m^{OL}$  and  $a_D^* - 2r_m^{OL}$  relationships may be expressed as follows -

$$a_D = \alpha(2r_m^{OL})^\beta \quad (6)$$

$$a_D^* = (2r_m^{OL})^{\beta'} \quad (7)$$

where exponents  $\beta$  and  $\beta'$  lie in the range of 1 to 2.5.

In addition to the  $2r_m^{OL}$ , the overloading cyclic plastic zone  $2r_C^{OL}$  is considered to be of significant importance as the zone of residual compressive stress field at the crack tip is determined by the length of this plastic zone. The  $2r_C^{OL}$  was computed using the relationships,

$$2r_C^{OL} = p(\Delta K_{OL}/2Y_s)^2 \quad (8)$$

where  $p = 1/\pi$  for plane stress,  $1/2\pi$  for mixed stress and  $1/3\pi$  for plane strain.

The logarithmic relationships were obtained as:

$$a_D \text{ (or } a_D^*) = m(2r_C^{OL})^n \quad (9)$$

where  $m$  and  $n$  are constants for a given alloy. In addition, the data points from literature were also analysed to find the trend. It is interesting to note that the exponent  $n$  lies in the range of 1 to 2.5 for both the  $a_D$  and  $a_D^*$  which is same as the value of exponent in  $a_D(a_D^*) - 2r_m^{OL}$  relationships.

The data points from literatures for various alloys as well as from the present investigation were analysed to get a comparative idea of the size scale of  $a_D$  and  $a_D^*$  against  $2r_m^{OL}$  and  $2r_C^{OL}$ . For a wide ranging alloys this relation may be expressed as,

$$a_D \approx (8 \text{ to } 35) \cdot 2r_C^{OL} \quad (10)$$

$$a_D^* \approx (1 \text{ to } 3.0) \cdot 2r_C^{OL} \quad (11)$$

$$a_D = (1 \text{ to } 3) \cdot 2r_m^{OL} \quad (12)$$

$$a_D^* = (0.1 \text{ to } 0.5) \cdot 2r_m^{OL} \quad (13)$$

It appears, therefore, that  $a_D$  is substantially larger than the  $2r_C^{OL}$  whereas  $a_D^*$  is comparable to this.

Based on the finding from the present work, schematic diagram comprising different plastic zones and retardation zones existing at the overload crack tip with their comparative size scales are presented in Fig. 6.

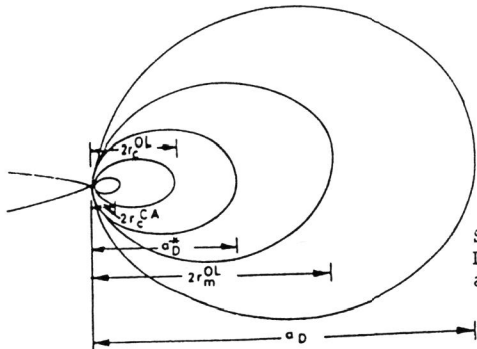


Fig. 6 Schematic Representation of Retardation Zones and Plastic Zones ahead of a crack Tip

Characterization of Retardation Zone

In the post overloading condition, the crack grows under the influence of a large compressive residual stress field created by overload plastic zone. Therefore, the FCGR is significantly low. However, once the crack tip comes out of compressive residual stress field, the FCGR relatively increases though still it does not acquire the preoverload growth rate. The crack closure effects are considered to be most pronounced in the overload cyclic plastic zone as the maximum level of compressive residual stresses are present in this zone. A typical compressive residual stress distribution (Matsuoka et al., 1978) (Fig. 7) reveals that the size of residual compressive stress field is about 2.5 times the overload cyclic plastic zone. Also, the highest level of compressive stress is attained generally over the

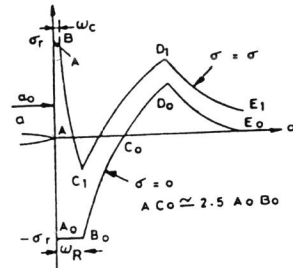


Fig. 7

Schematic Illustration of Stress Distribution and Plastic Zone after Application of Overload

length of cyclic plastic zone. In this aspect, the finding from the present work that  $a_D^* = (1 \text{ to } 3) \cdot 2r_C^{OL}$  makes interesting observation connoting that the size of  $a_D^*$  may vary from the zone of highest compression region (i.e.  $2r_C^{OL}$ ) to the zone over which the compressive stresses are present ahead of the crack tip. Since high compressive stresses are also indicative of high  $K_{op}^{OL}$  value, a significant role of  $K_{op}^{OL}$  on  $a_D^*$  may be appreciated.

CONCLUSIONS

1. The size of overload induced CGA zone increases with OLR and R in both the alloys and the micromechanism of crack growth is by formation of microvoids, tear ridges and dimples.
2. The crack growth rate in CGA zone increases with OLR and  $\Delta K$ . A typical increase in crack growth rate of the order of 2 to 3 is noticed on changing the OLR by a factor of two.
3. The retardation zone,  $a_D$  is found to increase with OLR (and  $K^{OL}$ ) and beyond a limiting level of OLR (or  $K^{OL}$ ) a tendency of saturation is noticed. The saturation tendency is linked with  $K_{op}^{OL}$  maxima.
4. The retardation zones  $a_D$  and  $a_D^*$  are related to the overload monotonic plastic zone size in the following manner:  $a_D$  (or  $a_D^*$ ) =  $\alpha$  (or  $\alpha'$ )  $\cdot (2r_m^{OL})^\beta$  (or  $\beta'$ ), where exponents  $\beta$  and  $\beta'$  lie in the range of 1-2.5. A similar relationship is found between  $a_D$  and  $a_D^*$  with overload cyclic plastic zone.
5. The size scales of  $a_D$  and  $a_D^*$  for wide ranging alloys were compared against plastic zone sizes  $2r_m^{OL}$  and  $2r_C^{OL}$  and following relations were noticed:
 
$$a_D = (1 \text{ to } 3) \cdot 2r_m^{OL}, \quad a_D^* = (8 \text{ to } 35) \cdot 2r_C^{OL}$$

$$a_D^* = (1-3) \cdot 2r_C^{OL}, \quad a_D = (0.1 \text{ to } 0.5) \cdot 2r_m^{OL}$$
6. The  $a_D^*$  is related to the zone of compressive residual stress field and so with the closure parameter  $K_{op}^{OL}$ .

## REFERENCES

- Bathias, C. and M. Vancon (1978). Mechanism of overload effect on fatigue crack propagation, Engng. Fracture Mech., 10, 409.
- Drew, M. et al. (1982). The effect of overload on fatigue crack propagation in offshore structural steel, Int. Conf. on Strength of Metals and Alloys, 2, 867.
- Matsuoka, S. and K. Tanaka (1978). Delayed retardation phenomenon of fatigue crack growth resulting from single overload, Engng. Fracture Mech., 10, 515.
- Ranganathan, N. et al. (1979). On contribution to the study of fatigue crack retardation in vacuum, Engng. Fracture Mech., 11, 775.
- Ranganathan, N. et al. (1984). On the influence of the initial K level on the post overload crack propagation behaviour, In Advances in Fracture Research, ICF6, 3, 1767.
- Robin, C. et al. (1983). Influence of an overload on the fatigue crack growth in steels, Fatigue of Engng. Mats. and Structures, 6, 658.
- Vardar, O. (1988). Effect of single overload in fatigue crack propagation, Engng. Fracture Mech., 30, 329.
- Verma, B.B. (1993). Effects of Overloading Cycle on Fatigue Crack Closure and Crack Growth Kinetics in Al-Alloy and Steel, Ph.D. Thesis, IIT Delhi, India.
- Wardclose, C.M. et al. (1989). Mechanism associated with transient fatigue crack growth, Engng. Fracture Mech., 32, 613.
- Willenborg, J. et al. (1971). Influence of stress state on crack growth retardation, ASTM, STP 924, 157.
- Wheeler, O.E. (1972). Spectrum loading and crack growth, J. Basic Engng., Trans. ASME, D94, 1812.